Chalcogenide Letters Vol. 22, No. 11, November 2025, p. 929 - 937

Synthesis and Characterization of Cu_2ZnSnS_4 (CZTS) Thin Films for Gas Sensor Applications

F. T. Ibrahim[1,*], A. A. Qassim[2] and S. M. A. Al-Dujayli[1]

[1]Physics Department, College of Science, University of Baghdad, Baghdad, 10071, Iraq
[2]College of Dentistry, Ibn Sina University of Medical and Pharmaceutical science, Baghdad, 21418, Iraq
*Corresponding Author: F. T. Ibrahim. Email: fuad.ibrahim@sc.uobaghdad.edu.iq

Received: 22 June 2025; Accepted: 3 November 2025

ABSTRACT: This work, pulse laser deposition technique was employee to synthesize Cu_2ZnSnS_4 (CZTS) thin films with different lasing energy (500, 600, 700, 800, 900 mJ). Through using different characterization technique to study structural, optical and gas sensing properties. the use of X-ray diffraction, the samples have polycrystalline with cubic structure. The EDX examination showed that the sample contains a suitable amount of Zn, Sn, Cu, and S atoms to form CZTS. UV-VIS measurement indicates that the synthesis of thin films employing a lower laser energy result in a drop in deposit sample thickness, which in turn reduces absorption and raises transmission. The electrical characteristics of CZTS thin films reveal that the mobility was decreased at 900 mJ, while the resistivity and carrier concentration were improved. The tested devices' gas response to ammonia (NH_3) and nitrogen dioxide (NO_2) gases at varying operation temperatures was conducted. The results showed that the sample had a sensitivity of up to 37.57% at 200°C for NH_3 gas, while the sample had a sensitivity of up to 52% at 300°C for NO_2 gas.

KEYWORDS: CZTS; pulse laser deposition; gas sensor; NO_2 gas; NH_3 gas

1 Introduction

CZTS, a quaternary sulfide with the formula Cu_2ZnSnS_4, is compound of copper (Cu), tin (Sn), zinc (Zn), and sulfur (S). CZTS is a semiconducting substance that can tolerate temperatures up to 800°C [1] and possesses p-type conductivity [2]. It was first proposed as an adsorbing material to replace the costly and limited elements of $Cu(In,Ga)Se_2$ (CIGS) in optoelectronic solar cells. In fact, CZTS performs well at harvesting light, with an ideal band gap energy of 1.5–1.6 eV [3], which is provided by valence and conduction bands at −3.8 and −5.2 eV, respectively [4]. Based on CZTS solar cells' external quantum efficiency, light-harvesting begins at a wavelength of approximately 400 nm and continues until it reaches over 800 nm [5]. Since the late 2000s, there has been a growing interest in the quaternary semiconducting compound copper zinc tin sulfide (CZTS) for use in thin-film solar cells [6]. Other materials, such as the sulfur-selenium alloy CZTSSe and copper zinc tin selenide (CZTSe), are included in the family of related materials [7]. Similar to copper indium gallium selenide (CIGS), CZTS has advantageous optical and electrical characteristics that make it a good choice for utilized in solar cells as an absorber layer. However, not similar CdTe or other thin films like CIGS, CZTS is made up entirely of plentiful and non- poisonous materials. The cost and accessibility of tellurium in CdTe and indium in CIGS, with the toxicity of cadmium, have been major factors in the quest for substitute materials for optoelectronic applications.

As of right now, a assortment of chemical and physical methods has been utilized to synthesis CZTS thin films for use as light absorbers. These methods include, radio frequency magnetron sputtering [8], hybrid thermal evaporation and sputtering [9], atom beam sputtering [10], pulsed laser deposition [11], spray pyrolysis technique [12], sol–gel spin technique, spray pyrolysis with ultrasonic, electrodeposition, and more.

In the present study, CZTS nanostructure thin films were synthesized as gas sensors on glass substrates using the pulse laser deposition method. There nanostructure, optical, electrical and gas sensing test on ammonia and nitrogen dioxide gases

https://doi.org/10.15251/CL.2025.2211.929

2 Experimental Procedure

Although a deposition system with the aforementioned characteristics can be expensive to buy, in this article, a multipurpose thin-film deposition system employing as PLD. The bell jar of glass with stainless steel base used ad vacuum chamber were contained a rotating multitarget holders, rotating substrate holder, and controller module for target position are basically the system's key components.

The Q-switched Nd:YAG laser system and a vacuum chamber evacuated to pressure (10^{-2} mbar) forming the PLD technique. The concentrated Nd: YAG laser beam, which has a power of around 500–900 mJ, enters through a ball jar wall and strikes the target's surface at a 45° angle. The target is positioned in front of the substrate, with its surface parallel to it. The substrate and the target are kept at an appropriate distance to avoid the substrate holder obstructing the incident laser beam. The solid-state Nd:YAG laser utilized for the deposition conditions had a 1064 nm wavelength, a repetition frequency of 6 Hz, and a pulse width of 10 ns. Ten centimeters separated the target from the laser source, while one to two centimeters separated it from the substrate.

Highly pure (99.99%) powders of zinc sulphite (ZnS), copper sulphite (CuS) and Tin sulphite (SnS). The pellet compose of 25% powders of zinc sulphite (ZnS),50% copper sulphite (CuS) and 25% Tin sulphite (SnS). To create a pellet that was 1 cm in diameter and 0.2 cm thick, the powders were combined and compressed for 10 min using a SPECAC hydraulic piston under 5 t of pressure. After being sintered in air for three hours at 500°C, these pellets were allowed to cool to ambient temperature.

The furnace's sintering temperature was raised at a rate of 10°C per minute. After cleaning the glass substrate with distilled water to get rid of any contaminants, it was cleaned for 15 min with alcohol and ultrasonic waves to get rid of grease and other impurities. Soft paper was used to wipe them after they had been dried by blowing air.

A handmade gas-detection system was employed for evaluating the sensors' sensing competence. The base plate was utilized for connecting electrical feeds. The base plate's heating was modified to heat the test sample and bring it up to the appropriate temperatures for operation. A thermocouple was utilized for recording the sensors' working temperature. A gas inlet gate was connected to one of the base plate's apertures, and electronic temperature monitors were connected to the thermocouple's output. A gas flow meter was used to provide the system with a known quantity of test gas in order to achieve the required gas concentration. A steady voltage and current were applied to the sensors.

The Shimadza-6000 X-ray diffractometer and an EDS detector (EDX-7000/8000, Shimadzu Corporation, Japan) were imploded to study the structural properties of nanocomposites films. For the prepared sample, FTIR (SHIMADZU-8400S) was used to make a scan of the FTIR measurements spanning the 400–4000 cm^{-1} range. A dual beam with a wavelength range of 0.19–1.1 μm was utilized to test the UV absorption using a Perkin Elmer Spectrophotometer Model Lambda 365.

3 Results and Discussion

Fig. 1 demonstrate X-ray diffraction (XRD) pattern, where, The CZTS samples were annealed at 200°C for two hours. A mixture of cubic structure (appears at peaks 2θ = ~33.2°, ~38.5°, ~55.7°, and ~66.3°) and tetragonal structure (distinctive peaks at 2θ = ~38.5°) [13] peaks appeared. When CZTS nanocrystals are very small, they can be either cubic or hexagonal. As they get bigger, they only show cubic crystals, which eventually transform into the thermodynamically stable tetragonal form [14].

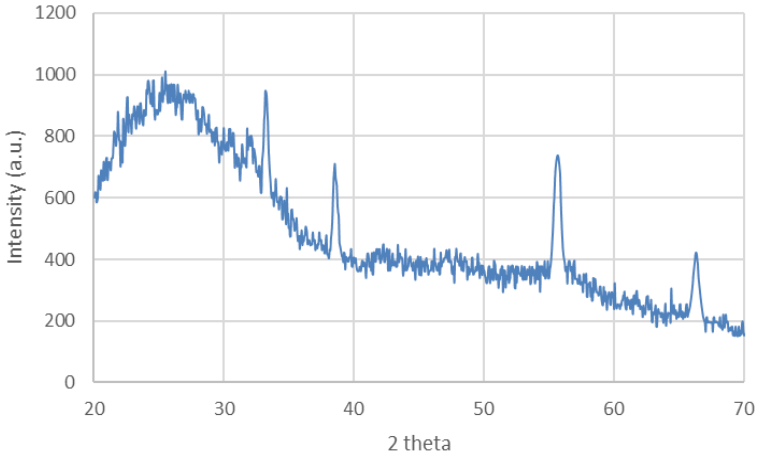

Figure 1: XRD spectra of CZTS thin films treated at 200°C.

Fig. 2: The structural characteristics of materials are measured employing energy dispersive X-ray spectroscopy (EDX). These figures display the film EDX spectra that were prepared. According to the EDX analysis, the sample comprises Zn, Sn, Cu, and S atoms; the weight ratios of each element are displayed in Table 1 of Ref. [15]. The result shows many peaks corresponding to CZTS elements and small amounts of O, N, and C elements considered as impurities were identified in the spectrum, these small amount of impurity's confirming the good purity and quality of the CZTS thin films [16].

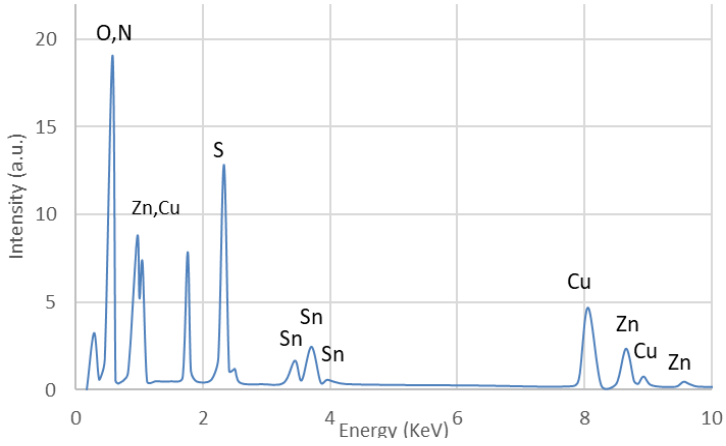

Figure 2: The EDX spectrum and atomic percentage of CZTS sample.

Element	Atomic %
C	9.0
N	2.1
O	23.1
S	26.0
Cu	19.1
Zn	12.2
Sn	8.5

Materials' structural characteristics are analyzed using Fourier Transform-Infrared (FTIR). Fig. 3 displays the FTIR spectra of the CZTS thin film that was placed on a glass substrate in the 400–4000 cm^{-1} wavenumber range. The O-H stretching is indicated by the high peak at 3101 to 3672 cm^{-1}. The appearance of an OH peak may be explained by the sample's moisture content or the conditions around it during the test. The OH peak may appear in the spectrum as a result of interactions between the molecule and the moisture. For as-synthesized materials, a faint metal sulfide band is also discernible in the 550–400 cm^{-1} area [17]. The synthesized CZTS samples, however, did not exhibit the distinctive peaks for the ZnS band [17] at about 600 cm–1, indicating the lack of subsequent phases.

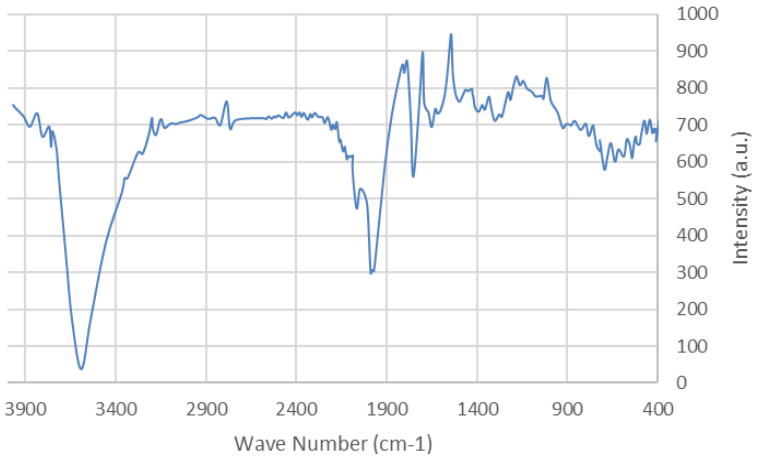

Figure 3: The FTIR spectrum of prepared CZTS.

The ultraviolet–visible (UV–vis) spectroscopy data with varying lasing energies (500, 600, 700, 800, and 900 mJ) are displayed in Fig. 4. The transmittance of the 500 mJ CZTS thin film is higher than that of the 900 mJ. Beer-Lambert's law states that a material's transmittance will rise as its thickness decreases since it will absorb less [18]. This outcome demonstrates that the CZTS film will be thinner at lower lasing energies. The insert of Fig. 5 displays Tauc's plot of CZTS thin films with varying laser energy. For CZTS thin films, the band gaps were approximately 1.65 and 1.75 eV, respectively.

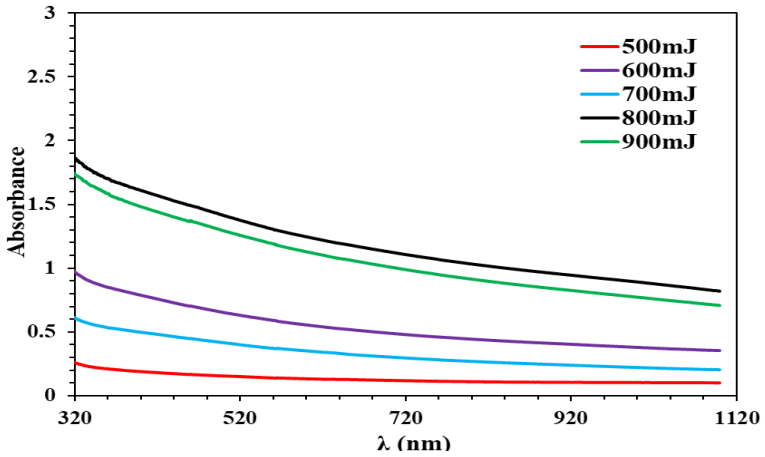

Figure 4: The absorbance spectrum of CZTS with different laser deposition energy.

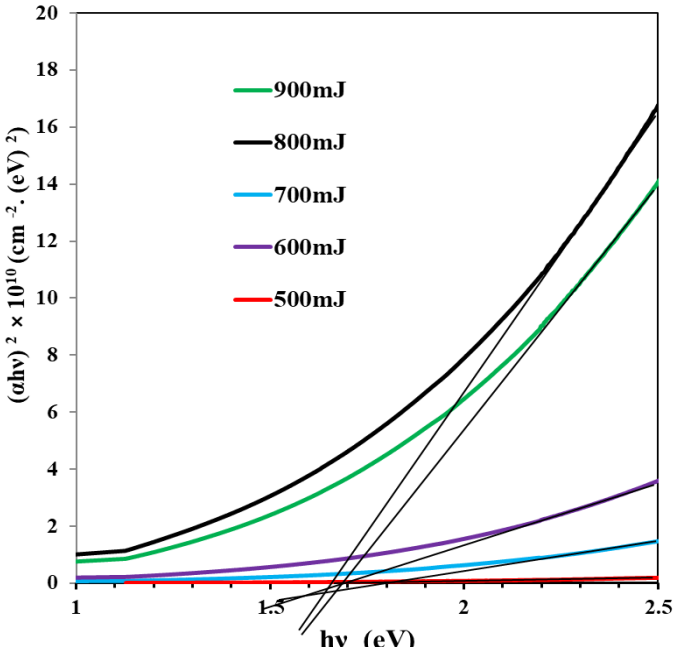

Figure 5: The optical energy gap measurement of CZTS with different laser deposition energy.

Although the acquired band gaps remained consistent with the CZTS band gap range reported in the literature, the thicker CZTS thin film that was deposited may be responsible for the band gap's reduction with increasing concentration. It is possible that the film contains structural flaws that could lead to localized states close to the conduction band. The bandgap may be reduced in thick films as a result of these localized states merging with the conduction band [19].

The hall parameters of CZTS thin films were measured at varying laser energy (500 mJ, 700 mJ, 900 mJ) by Hall effect measurements. The results for CZTS thin films coated on glass are displayed in Table 1. With an increase in laser energy, the resistivity value rises noticeably. Microstructures and phase transitions are known to affect CZTS's electrical characteristics. High laser energy promotes grain growth and refinement, which lowers the quantity of defects [20], and tetragonal CZTS has a lower resistivity than other CZTS phases [21]. The significant variation in resistivity and carrier concentration, however, most likely results from a challenging structure created by the laser deposition process.

Table 1: Hall effect parameters of CZTS thin films with varying laser energy.

Specimen	Thickness (nm)	Resistivity (Ω·cm)	Carrier Concentration (cm^{-3})	Carrier Mobility (cm^2/Vs)
500 mJ	~190	4.0×10^7	6×10^{22}	27
700 mJ	~300	4.6×10^7	1×10^{22}	21
900 mJ	~435	4.8×10^7	1×10^{21}	17

The carrier concentration and resistivity measured at 900 mJ were better when the mobility was lower. The secondary phase and microstructure have already been found to have a significant impact on carrier movement [22]. Because the two factors are inversely proportional, removing the SnS secondary phase will increase carrier mobility, which will further lower the resistivity and enhance the CZTS thin film's overall electrical properties.

The operating temperature was varied (200, 250, 300) °C, where an oxidizing gas such as (NO_2) and reducing gas (NH_3) at concentration of 60 ppm and 30 ppm used as test gases respectively. In Fig. 6 shows the sensitivity of the samples prepared at (900 mJ) deposited on glass substrate. its notes that the maximum sensitivity at 60 ppm NO_2 gas can reaches to 52% at around 300°C [23], while the maximum sensitivity to NH_3 gas was reaches to 37.57% at 200°C [24].

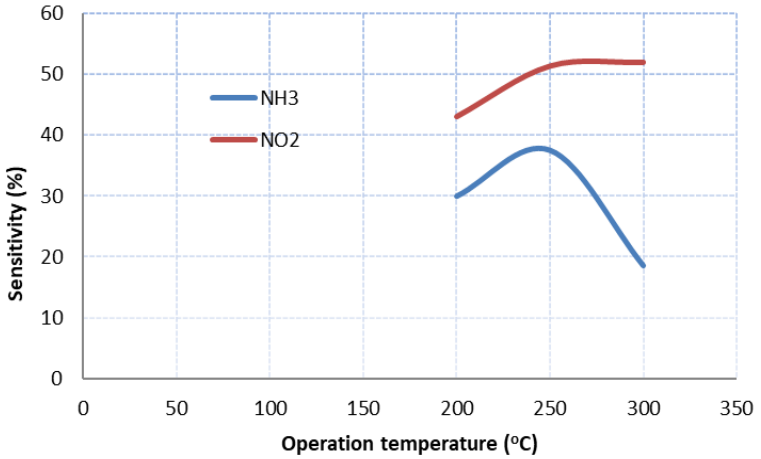

Figure 6: The CZTS sensitivity with temperature of operating to NO_2 gas and NH_3 gas.

As demonstrated by the previous findings, gas sensors' sensitivity to oxidizing and reducing gases has significantly increased. The nanoparticle on the glass substrate and the higher quantity of surface adsorbed oxygen species are the causes.

Figs. 7 and 8 show the response time and recovery time of gas sensors coated on glass substrates as a function of temperature for NO_2 and NH_3 gases. The successive tests were performed at an operation temperature 200–300°C operating temperature. The results are shown in Fig. 7 the response time decrease with increased the operation temperature show the have 25.2 s a higher response time as at 250°C and have 57 s a higher recovery time to NH_3 gas at 300°C.

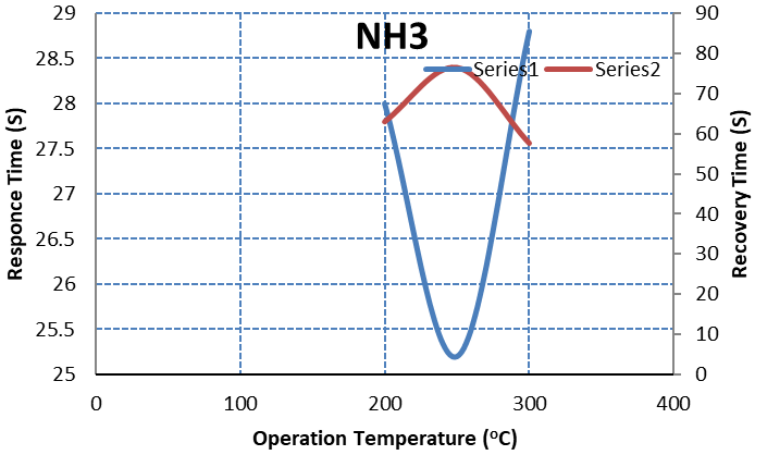

Figure 7: The CZTS response and recovery time with temperature of operating to NH3 test gas.

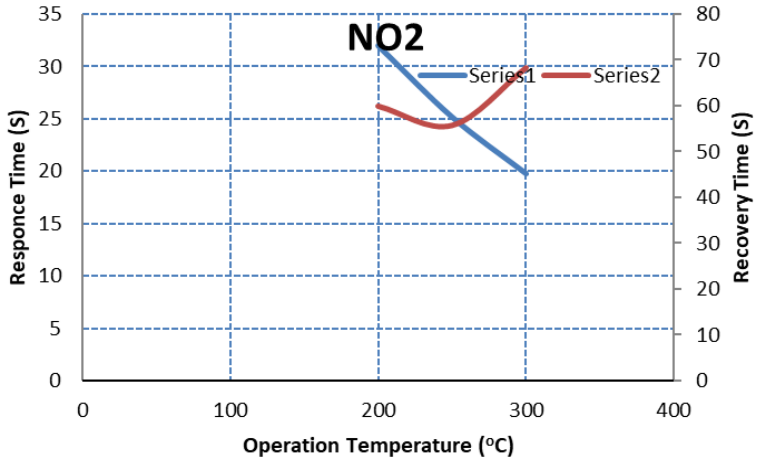

Figure 8: The CZTS response and recovery time with temperature of operating to NO_2 test gas.

Fig. 8 shows the results the response and recovery time of gas sensor sample, where, the response and recovery time decrease with increased the operation temperature. The has 52.2 s a higher recovery time gas at 250°C.

4 Conclusion

This work had clearly shown how to use pulse laser deposition technique to synthesize CZTS nanostructure. The behavior of the thin films, as demonstrated by the provided graphs, indicated that the films were suitable for use as an NH_3 and NO_2 gases sensing device due to their enhanced sensitivity, low reaction time, and recovery time.

Acknowledgement: I would like to thank University of Baghdad for their support in finishing this research.

Funding Statement: This work was supported by ongoing institutional funding. No additional grants to carry out or direct this particular research were obtained.

Author Contributions: Each co-author has made unique contributions to the work. The author F. T. Ibrahim prepared the thin films and contriuted to writing the article. S. M. A. Al-Dujayli wrote the program for gas sensor properties. As the author A. A. Qassim, he supervised the work, contributed to the analysis of the results. And reviewed the article draft.

Availability of Data and Materials: Data sharing is not applicable to this article as no datasets were created or analyzed during the current study.

Ethics Approval: The authors would like to declare that they do not have any conflict of interests.

Conflicts of Interest: The authors of this work declare that they have no conflicts of interest.

References

1. Kattan N, Hou B, Fermín DJ, Cherns D. Crystal structure and defects visualization of Cu_2ZnSnS_4 nanoparticles employing transmission electron microscopy and electron diffraction. Appl Mater Today. 2015;1:52–9. https //doi.org/10.1016/j.apmt.2015.08.004.
2. Nakayama N, Ito K. Sprayed films of stannite Cu_2ZnSnS_4. Appl Surf Sci. 1996;92:171–5. https://doi.org/10.1016/0169-4332(95)00225-1.
3. Gonce MK, Dogru M, Aslan E, Ozel F, Patir IH, Kus M, et al. Photocatalytic hydrogen evolution based on Cu_2ZnSnS_4, $Cu_2ZnSnSe_4$ and $Cu_2ZnSnSe_{4-x}S_x$ nanofibers. RSC Adv. 2015; 5:94025–8. https://doi.org/10.1039/c5ra18877f.
4. Huang S, Luo W, Zou Z. Band positions and photoelectrochemical properties of Cu_2ZnSnS_4thin films by the ultrasonic spray pyrolysis method. J Phys D Appl Phys. 2013; 46:235108. https://doi.org/10.1088/0022-3727/46/23/235108.
5. Park S-N, Sung S-J, Sim J-H, Yang K-J, Hwang D-K, Kim J, et al. Nanostructured p-type CZTS thin films prepared by a facile solution process for 3D p–n junction solar cells. Nanoscale. 2015;7:11182–9. https://doi.org/10.1039/c5nr02081f.
6. Zhang X, Fu E, Wang Y, Zhang C. Fabrication of Cu_2ZnSnS_4 (CZTS) Nanoparticle Inks for Growth of CZTS Films for Solar Cells. Nanomaterials. 2019;9:336. https://doi.org/10.3390/nano9030336.
7. Sadewasser S., et al. Thin Solid Films. 2006;361(6):1. https://doi.org/10.1002/pssa.200669573.
8. Abdallah B, Mrad O, Ismail I. Characterization of TiAlV films prepared by vacuum arc deposition: effect of substrate temperature. Acta Phys Pol A. 2013;123:76–9. https://doi.org/10.12693/aphyspola.123.76.
9. Kathirvel D, Suriyanarayanan N, Prabahar S, Srikanth S. Structural, electrical and optical properties of cds thin films by vacuum evaporation deposition. *J Ovonic Res.* 2011:7(4):83.
10. Hassan RAH, Ibrahim FT. Preparation and characterization of anatase titanium dioxide nanostructures as smart and self-cleaned surfaces. Iraqi J Appl Phys. 2020;16(4):13–8.
11. Ibrahim FT. Annealing effects on optical and structural properties of chromium oxide thin film deposited by PLD technique. *Iraqi J Phys.* 2018;16:35–41. https://doi.org/10.30723/ijp.v16i38.7.
12. Alborisha MAS, Ibrahim FT, Jilani W, Bouzidi A, Guermazi S. Investigations on TiO_2–NiO@In_2O_3 nanocomposite thin films (NCTFs) for gas sensing: synthesis, physical characterization, and detection of NO_2 and H_2S gas sensors. J Mater Sci. 2024;59:3451–66. https://doi.org/10.1007/s10853-024-09376-z.
13. Unveroglu B, Zangari G. Photoelectrochemical behavior of bismuth-containing Cu_2ZnSnS_4(CZTS) absorber layers for photovoltaic applications. J Electrochem Soc. 2018; 166:H3040–H3046. https://doi.org/10.1149/2.0081905jes.
14. Tong Z, Yan C, Su Z, Zeng F, Yang J, Li Y, et al. Effects of potassium doping on solution processed kesterite Cu_2ZnSnS_4 thin film solar cells. Appl Phys Lett. 2014;105:223903. https://doi.org/10.1063/1.4903500.
15. Vanalakar S, Agawane G, Shin S, Suryawanshi M, Gurav K, Jeon K, et al. A review on pulsed laser deposited CZTS thin films for solar cell applications. J Alloys Compd. 2015; 619:109–21. https://doi.org/10.1016/j.jallcom.2014.09.018.
16. Song X, Ji X, Li M, Lin W, Luo X, Zhang H. A review on development prospect of CZTS based thin film solar cells. Int J Photoenergy. 2014;2014:1–11. https://doi.org/10.1155/2014/613173.
17. Indubala E, Sarveshvaran S, Sudha V, Mamajiwala AY, Harinipriya S. Secondary phases and temperature effect on the synthesis and sulfurization of CZTS. Sol Energy. 2018; 173:215–24. https://doi.org/10.1016/j.solener.2018.07.085.
18. Su C-Y, Kuo T-W, Chen P-C, Chiu Y-C, Lin P-C, Chang C-C. Preparation and characterization of CZTS target and thin film using multi-stage hot-pressing process and pulsed laser deposition. Ceram Int. 2018;44:S96–S99. https://doi.org/10.1016/j.ceramint.2018.08.231.
19. Calvet I, Barrachina E, Martí, R, Fraga D, Lyubenova TS, et al. Synthesis, deposition and crystal growth of CZTS nanoparticles onto ceramic tiles. Boletin De La Soc Espanola De Ceram Y Vidr. 2015;54:175–80. https://doi.org/10.1016/j.bsecv.2015.09.003.
20. Ghediya PR, Chaudhuri TK, Vankhade D. Electrical conduction of CZTS films in dark and under light from molecular solution ink. J Alloys Compd. 2016;685:498–506. https://doi.org/10.1016/j.jallcom.2016.05.299.

21. Al-Shakban M, Matthews PD, Savjani N, Zhong XL, Wang Y, Missous M, et al. The synthesis and characterization of Cu2ZnSnS4 thin films from melt reactions using xanthate precursors. J Mater Sci. 2017;52:12761–71. https://doi.org/10.1007/s10853-017-1367-0.
22. Shin SW, Pawar S, Park CY, Yun JH, Moon J-H, Kim JH, et al. Studies on Cu_2ZnSnS_4 (CZTS) absorber layer using different stacking orders in precursor thin films. Sol Energy Mater Sol Cells. 2011;95:3202–6. https://doi.org/10.1016/j.solmat.2011.07.005.
23. Wang Y, Fu X, Wang T, Li F, Li D, Yang Y, et al. Polyoxometalate electron acceptor incorporated improved properties of Cu_2ZnSnS_4-based room temperature NO_2 gas sensor. Sensors Actuators B Chem. 2021;348:130683. https://doi.org/10.1016/j.snb.2021.130683.
24. Gurav K, Shin S, Patil U, Deshmukh P, Suryawanshi M, Agawane G, et al. Cu_2ZnSnS_4 (CZTS)-based room temperature liquefied petroleum gas (LPG) sensor. Sensors Actuators B Chem. 2014;190:408–13. https://doi.org/10.1016/j.snb.2013.08.064.